Transition Probabilities in ^{134}Pr: A Test for Chirality in Nuclear Systems

D. Tonev,[1,2] G. de Angelis,[1] P. Petkov,[2] A. Dewald,[3] S. Brant,[4] S. Frauendorf,[5] D. L. Balabanski,[2,6] P. Pejovic,[3]
D. Bazzacco,[7] P. Bednarczyk,[8] F. Camera,[9] A. Fitzler,[3] A. Gadea,[1] S. Lenzi,[7] S. Lunardi,[7] N. Marginean,[1] O. Möller,[3]
D. R. Napoli,[1] A. Paleni,[9] C. M. Petrache,[6] G. Prete,[1] K. O. Zell,[3] Y. H. Zhang,[10] Jing-ye Zhang,[11]
Q. Zhong,[12] and D. Curien[8]

[1]*Laboratori Nazionali di Legnaro, INFN, I-35020 Legnaro, Italy*
[2]*Institute for Nuclear Research and Nuclear Energy, BAS, 1784 Sofia, Bulgaria*
[3]*Institut für Kernphysik der Universität zu Köln, D-50937 Köln, Germany*
[4]*Department of Physics, Faculty of Science, University of Zagreb, 10000 Zagreb, Croatia*
[5]*Department of Physics, University of Notre Dame, Notre Dame, Indiana 46556, USA*
[6]*Dipartimento di Fisica, Università di Camerino and INFN Perugia, I-62032 Camerino, Italy*
[7]*Dipartimento di Fisica, Università and INFN Sezione di Padova, I-35131 Padova, Italy*
[8]*Institut de Recherches Subatomiques, Boîte Postale 28 F-67037, Strasbourg, France*
[9]*Dipartimento di Fisica, Università di Milano, I-20133 Milano, Italy*
[10]*Institute of Modern Physics, Chinese Academy of Sciences, Lanzhou 73000, Peoples Republic of China*
[11]*Department of Physics and Astronomy, University of Tennessee, Knoxville, Tennessee 37996, USA*
[12]*Department of Nuclear Physics, China Institute of Atomic Energy, Beijing 102413, Peoples Republic of China*

Exited states in ^{134}Pr were populated in the fusion-evaporation reaction ^{119}Sn(^{19}F, $4n$)^{134}Pr. Recoil distance Doppler-shift and Doppler-shift attenuation measurements using the Euroball spectrometer, in conjunction with the inner Bismuth Germanate ball and the Cologne plunger, were performed at beam energies of 87 MeV and 83 MeV, respectively. Reduced transition probabilities in ^{134}Pr are compared to the predictions of the two quasiparticle + triaxial rotor and interacting boson fermion-fermion models. The experimental results do not support the presence of static chirality in ^{134}Pr underlying the importance of shape fluctuations. Only within a dynamical context the presence of intrinsic chirality in ^{134}Pr can be supported.

Chirality has recently been proposed as a novel feature of rotating nuclei [1–3]. A spontaneous breaking of the chiral symmetry can take place for configurations where the angular momenta of the valence protons, valence neutrons, and the core are mutually perpendicular. This can occur, for example, when the proton and neutron Fermi levels are located in the lower part of valence proton high-j (particlelike) and in the upper part of valence neutron high-j (holelike) subshells, and the core is triaxial. Under such conditions the angular momenta of the valence particles are aligned along the short and long axes of the triaxial core, while the angular momentum of the rotational core is aligned along the intermediate axis. The nonzero components of the total angular momentum on all the three axes can form either a left-handed or a right-handed set and therefore, the system manifests chirality [2]. Since the chiral symmetry is dichotomic, its spontaneous breaking by the axial angular-momentum vector leads to doublets of closely lying rotational bands of the same parity [1–3]. Recently, pairs of bands possibly due to the breaking of the chiral symmetry have been found in the mass $A \sim 130$ region where the proton Fermi surface is positioned in the lower part and the neutron surface in the higher part of the $h_{11/2}$ subshell. The first example of two nearly degenerate bands with the same parity and spins has been reported for ^{134}Pr [4,5]. The two bands are displayed in

Fig. 1. The degeneracy between levels of the same spin and parity increases with increasing spin and the bands cross above $I > 15\hbar$. In the context of chiral symmetry such a doublet of bands has been described within the framework of the particle-core coupling model [1,3] and the tilted-axis cranking model [2]. An alternative interpretation has been based on the interacting boson fermion-fermion model (IBFFM) [6]. Here the energy degeneracy is also obtained but a different nature is attributed to the two bands. The yrast band is basically built on the ground state configuration of the triaxial core whereas the collective structure of the yrare band contains a large component of the γ band and, with increasing angular momentum, of higher-lying collective core structures.

In order to confirm or reject the hypothesis of nuclear chirality, next to establish the existence of almost degenerate rotational bands, it is also necessary to measure other observables and compare them to the model predictions. Critical experimental observables for the understanding of nuclear structure and for checking the reliability of theoretical models are the electromagnetic transition probabilities. The aim of the present work is to investigate the electromagnetic transition probabilities in the doublet bands of ^{134}Pr.

Excited states in ^{134}Pr were populated using the reaction ^{119}Sn(^{19}F, $4n$)^{134}Pr. The beam was delivered by the
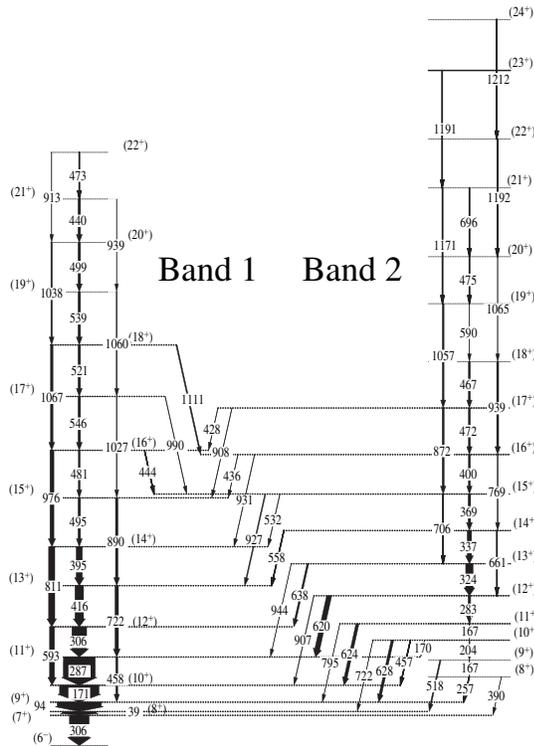
FIG. 1. Partial level scheme of ^{134}Pr from Ref. [16]. Two nearly degenerate positive-parity bands, candidates for chiral partner bands, are indicated as Band 1 and Band 2.

FIG. 2. Gated γ-ray spectra of ^{134}Pr taken at four different distances. The summed spectra from all detectors positioned at the backward angle of 137.60° with respect to the beam axis are shown. On the left-hand side, the shifted and unshifted components of the $11_1^+ \rightarrow 10_1^+$ transition are presented, on the right-hand side, the shifted and unshifted components of the $12_1^+ \rightarrow 10_1^+$ transition are shown.

Vivitron accelerator at IReS in Strasbourg. Lifetimes of the states were measured using both the recoil distance Doppler-shift (RDDS) and the Doppler-shift attenuation (DSAM) methods. For the RDDS measurement, a beam with an energy of 87 MeV was used. The target consisted of 0.5 mg/cm^2 ^{119}Sn evaporated on a 1.8 mg/cm^2 ^{181}Ta foil facing the beam. The recoils, leaving the target with a velocity of 0.98(2)% of the velocity of light, were stopped in a 6.0 mg/cm^2 gold foil. For the DSAM measurement, a beam energy of 83 MeV was used. The target consisted of 0.7 mg/cm^2 ^{119}Sn evaporated on a 9.5 mg/cm^2 ^{181}Ta backing used to stop the recoils.

The deexciting γ rays were detected using the EUROBALL IV detector array and an inner Bismuth Germanate (BGO) ball [7]. Events were collected when at least three γ rays in the Ge cluster or clover segments and three segments of the inner ball fired in coincidence. A standard add-back correction for Compton scattering was applied. In the RDDS case data were taken at 20 target-to-stopper distances ranging from electrical contact to 2500 μm. Examples of spectra taken at different distances for two γ-ray transitions in ^{134}Pr are shown in Fig. 2. For the analysis of the RDDS data, the standard version of the differential decay-curve method (DDCM) [8] has been employed, with gates set on both shifted (S) and unshifted (U) components of a transition depopulating levels below the level of interest. For each flight time t, a lifetime value
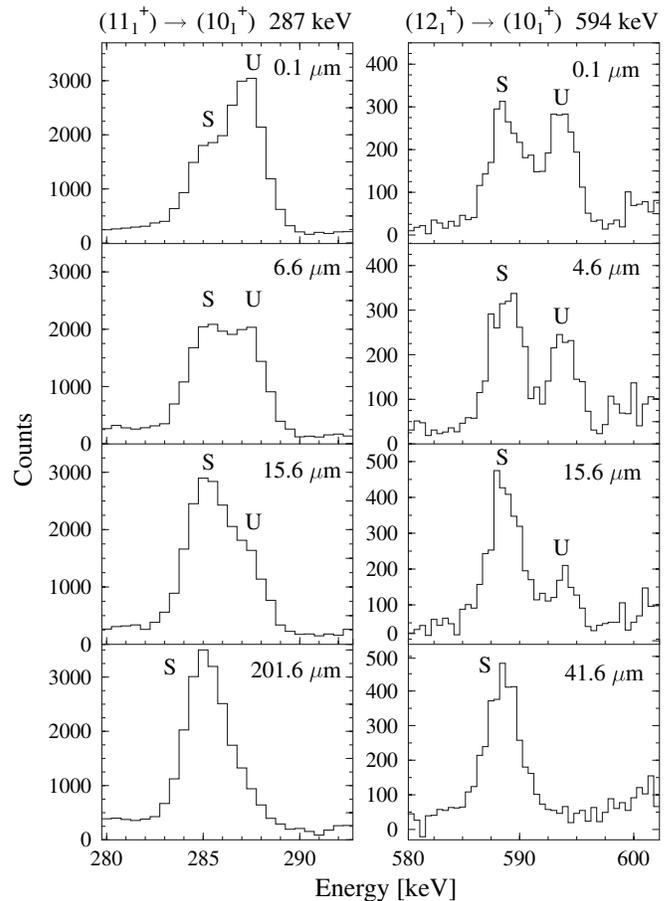
τ for the level of interest is calculated by directly using the areas of the U or S peaks of a transition depopulating the investigated level and of the directly feeding transitions. A lifetime value is derived at each distance and the final result for τ is determined as an average of such values within the sensitivity region of the data. More details about the DDCM applied to RDDS measurements can be found in Refs. [8,9]. For the analysis of the DSAM data, we performed a Monte Carlo simulation of the slowing-down histories of the recoils using a modified [10,11] version of the program DESASTOP [12]. The analysis of the line shapes was carried out according to the DDCM for treating DSAM data [9,10]. The lifetimes of the levels with I^π from 10_1^+ to 18_1^+ and with I^π from 13_2^+ to 17_2^+ have been deduced. Except for the lifetime of the $I^\pi = 10_1^+$ level [13], all the others are determined for the first time. We observe an excellent agreement with the lifetime value for the $I^\pi = 10_1^+$ state reported in Ref. [13]. The results are shown in the Table I. Almost all branching ratios reported in

TABLE I.   Derived lifetimes in Band 1 and Band 2 of ^{134}Pr.
The used experimental technique is also indicated.

Band 1			Band 2		
State (I^π)	τ (ps)		State (I^π)	τ (ps)	
10_1^+	4.93(15)	RDDS	13_2^+	1.443(50)	
11_1^+	1.614(326)	RDDS	14_2^+	1.280(50)	
12_1^+	1.425(130)	RDDS			
13_1^+	0.904(50)	RDDS			
$14_1^{+\,a}$	0.882(147)	DSAM	$15_2^{+\,a}$	0.887(47)	
15_1^+	0.608(68)	DSAM	16_2^+	0.824(52)	
16_1^+	0.562(47)	DSAM	17_2^+	0.353(49)	
17_1^+	0.422(30)	DSAM			
18_1^+	0.249(10)	DSAM			

^{a}The lifetimes for the states 14_1^+ and 15_2^+ have been determined
from both the RDDS and DSAM measurements. The results
show very good agreement within the error. In the table we
report only the DSAM results due to their higher statistical
significance.

Ref. [4] were revised. The clover rings of Euroball form a
highly efficient Compton polarimeter. We confirmed
that the delayed component of the 306 keV doublet has
an $E1$ character as already reported by Roberts *et al.* [14].
On the basis of directional correlation of γ radiation from
oriented states [4] and linear polarization analysis, an $M1$
character with a negligible $E2$ component was assigned to
the $\Delta I = 1$ intraband transitions. The $\Delta I = 2$ intraband
and interband transitions show an $E2$ character. Details of
the lifetime analysis, branching ratios and linear polariza-
tions coefficients will be reported in a forthcoming pub-
lication [15].

Reduced transition probabilities obtained from the
present experiment are shown in Fig. 3. Within the experi-
mental uncertainties, the $B(M1)$ values in both partner
bands behave similarly and point to relatively strong tran-
sition strengths. In contrast, the intraband $B(E2)$ strengths
within the two bands differ. In the angular-momentum
region where the almost degeneracy of the energy levels
of the two bands occurs ($I^\pi = 14^+$–19^+), the $B(E2)$ values
for Band 1 are a factor 2 to 3 larger than those of Band 2.
The $B(M1)/B(E2)$ ratios obtained from the lifetime data
are in a good agreement with the results extracted from
intensity values reported in Ref. [4] and differ only for
the $I^\pi = 13_1^+$ and 15_1^+ states from the values reported in
Ref. [16]. In all measurements the corresponding
$B(M1)/B(E2)$ ratios for the two bands are different. The
staggering in Band 1 reported in Ref. [16] is not observed
in our data as well as in the data of Ref. [4]. Our results are
incompatible with the pure chiral picture (static chirality)
where the intraband $B(E2)$ transition strengths must be
almost equal [1,17]. Such a finding points to the fact that
the limit of static chirality is not reached in ^{134}Pr and the
nucleus stays in a very soft vibrational regime.

In order to investigate the effects of the shape fluctua-
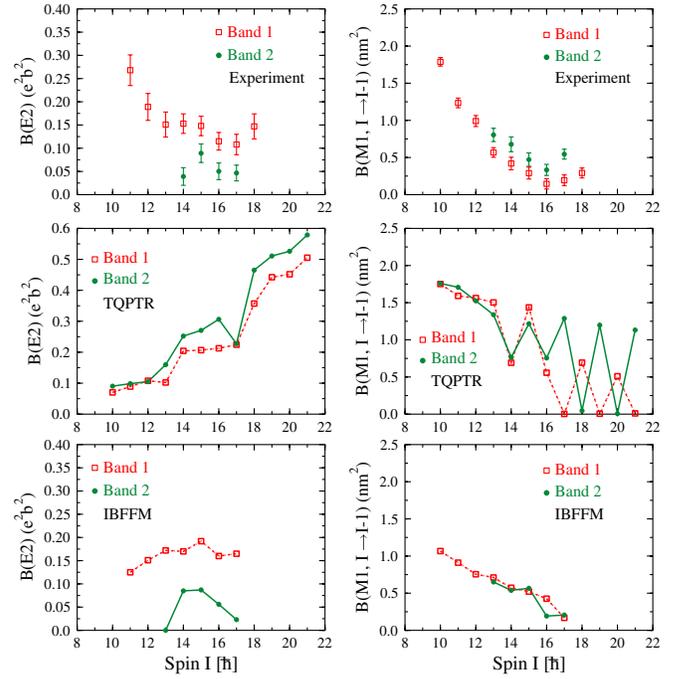tions we have compared the experimental transition

FIG. 3 (color online).   Experimentally determined and theoreti-
cally calculated $B(E2)$ and $B(M1)$ transition strengths in chiral
candidate bands of ^{134}Pr. In the upper panels experimental $B(E2)$
and $B(M1)$ values for transitions in Band 1 and Band 2 are
presented. In the second row, the results of TQPTR calculations
are displayed. In the panels on the bottom the predictions of the
IBFFM are presented.

strengths of the two bands with calculated ones by means
of the two quasiparticle + triaxial rotor (TQPTR) model
as described in Refs. [1,18] and by the IBFFM [6]. For the
TQPTR, the ratios between the moments of inertia have
been calculated by cranking about the three principal axes
using the parameters reported in Ref. [2], which give
$\mathcal{J}_s:\mathcal{J}_i:\mathcal{J}_l = 1.52:3.55:1$. In the IBFFM calculation, the
proton and neutron are coupled to the triaxial core as
described in Ref. [6]. Both descriptions include the
coupling between the odd particles and the even-even
core in a similar way, taking into account the partial filling
of the $h_{11/2}$ shells. In the TQPTR model, a rigid triaxial
shape is assumed for the core and the orientation in space is
the only core degree of freedom. The IBFFM takes into
account the deformation of the core as an additional de-
gree of freedom. As discussed in Ref. [6], a cubic term
had to be added to the standard interacting-boson ap-
proximation (IBA) Hamiltonian in order to reproduce the
energy spectra of ^{134}Pr and its even-even isobar ^{134}Ce. This
term generates a triaxial equilibrium deformation.
The fluctuations of the shape around this value are
taken into account and their magnitude is fixed by adjust-
ing the parameters for the IBA Hamiltonian to the data
for ^{134}Ce. The results of both calculations are shown in
Fig. 3. The comparison with the experimental data show a
clear disagreement with the TQPTR results whereas a

much better matching is found with the IBFFM calculation. Such results indicate that shape fluctuations are an essential ingredient for the proper description of the structure of the two bands. It is interesting to note that the difference of the transition strengths of the two bands is larger, and the theoretical values are closer to the experimental $B(E2)$ values in the IBFFM calculation than in the TQPTR one. This fact supports the interpretation of Ref. [6] where the yrast band contains predominantly the ground state configuration of the triaxial core whereas the yrare band contains a major component of the γ band. Such interpretation does not necessarily contradict the chiral interpretation, because the TQPTR calculations in Ref. [19] found a similar composition.

In the chiral interpretation the eigenstates of the Hamiltonian representing the two observed bands can be described as linear combinations of the wave functions in the left-handed and right-handed sectors. In the case of static chirality the overlap between the wave functions in the two sectors is weak. Because such coupling represents the tunneling between the two chiral configurations, the matrix elements of the electromagnetic transition operators between the two chiral sectors are expected to be very small. Since the left- and right-handed components enter with equal weight into the two eigenstates, which differ only in the relative phase of the mixing amplitudes, the transition matrix elements of the two doublet bands have to be equal. In the case of dynamic chirality, the overlap between the wave functions of the two sectors is large. In such a condition there are large matrix elements of the transition operators that connect the left- to the right-handed sector. Because of orthogonality, these matrix elements enter the transition matrix elements of the eigenstates with opposite sign and make the transition strengths of the two doublet bands different.

The TQPTR calculation shows a transition from dynamic to static chirality with increasing spin. Below $I^\pi = 12^+$, the angular-momentum vector oscillates between the left- and right-handed sectors, separated by the plane defined by the short and long axes (s-l). The two bands are well separated, representing the ground and first excited states of this chiral vibration [5]. Above $I^\pi = 12^+$, the angular momentum increases by adding core angular momentum perpendicular to the s-l plane. This reduces the probability of the angular-momentum vector to be near the s-l plane, which makes the electromagnetic transition matrix elements between the two sectors small. Static chirality is approached, which is reflected by the two partner bands coming close together. The $B(E2)$ values indicate that there is still a substantial tunneling between the two sectors. In the IBFFM model, the fluctuations of the triaxiality parameter γ around its mean value of 30° admix near-axial shapes, which are achiral. This additional left-right coupling strongly increases the difference between the intraband $B(E2)$ values. A pronounced staggering of the $B(M1)$

values appears above $I^\pi = 12^+$ in the TQPTR model. An explanation for this staggering was given in Ref. [17] for the symmetric case where the angular momenta of the proton and the neutron hole are equal, the moments of inertia of the l and s axes are equal, and the left-right transition matrix element is negligible. Our TQPTR calculation does not strictly obey these conditions, mainly because the microscopic moments of inertia of the long and short axes are different. The staggering is absent in the data as well as in the results of the IBFFM calculations, which indicates that the additional left-right coupling caused by the shape fluctuations cancels the staggering effect forseen in Ref. [17].

The assumption of a constant deformation of $\gamma = 30°$ in the TQPTR gives increasing $B(E2)$ transition strengths as a function of spin, which is in contrast to the observed trend. Such an increase of the $B(E2)$ transition strengths is directly related to the chiral geometry, which at low spins requires that the rotational axis lies in the plane defined by the short and long axes of the core, with an angle of 45° with respect to both of them. In such a situation the $B(E2)$ values are equal to zero. With increasing spin the angular momentum moves out of the plane which correspondingly increases the $B(E2)$ values. For axial shape instead the same geometry gives rise to large $B(E2)$ values. Therefore, the admixture of near-axial shapes will increase the $B(E2)$ values at low spin, which results in the almost constant values seen in Fig. 3 and foreseen by the IBFFM calculations.

In summary, our lifetime measurements and the theoretical analysis do not support static chirality in ^{134}Pr, as suggested on the basis of the similar energies of the two positive-parity bands [1]. The experimental $B(E2)$ values are larger in Band 1 than in Band 2 whereas the $B(M1)$ values are slightly larger in Band 2 than in Band 1. The experimental difference between the $B(E2)$ values cannot be reproduced assuming a rigid triaxial shape (TQPTR) which would also result in a pronounced staggering of the $B(M1)$ values not found in the experimental data. The experimentally observed transition matrix elements can be reproduced by taking into account the fluctuations of the nuclear shape (IBFFM). This means that the chirality in ^{134}Pr, if it exists, has mainly a dynamical character, the nuclear system fluctuating between chiral and achiral configurations, which couples the two sectors and generates the differences in the transition rates. Thereby the coupling due to shape fluctuations seems to play a central role. However, it may also indicate that the coupling of the two quasiparticles to the shape degrees of freedom is the prominent mechanism.

[1] S. Frauendorf *et al.*, Nucl. Phys. **A617**, 131 (1997).
[2] V. I. Dimitrov *et al.*, Phys. Rev. Lett. **84**, 5732 (2000).
[3] K. Starosta *et al.*, Nucl. Phys. **A682**, 375c (2001).
[4] C. M. Petrache *et al.*, Nucl. Phys. **A597**, 106 (1996).
[5] K. Starosta *et al.*, Phys. Rev. Lett. **86**, 971 (2001).
[6] S. Brant *et al.*, Phys. Rev. C **69**, 017304 (2004).
[7] J. Simpson, Z. Phys. A **358**, 139 (1997).
[8] A. Dewald *et al.*, Z. Phys. A **334**, 163 (1989).
[9] G. Böhm, A. Dewald, P. Petkov, and P. von Brentano, Nucl. Instrum. Methods Phys. Res., Sect. A **329**, 248 (1993).
[10] P. Petkov *et al.*, Nucl. Phys. **A640**, 293 (1998).
[11] P. Petkov *et al.*, Nucl. Instrum. Methods Phys. Res., Sect. A **431**, 208 (1999).
[12] G. Winter, Nucl. Instrum. Methods **214**, 537 (1983).
[13] T. Klemme *et al.*, Phys. Rev. C **60**, 034301 (1999).
[14] S. P. Roberts *et al.*, Phys. Rev. C **67**, 057301 (2003).
[15] D. Tonev *et al.*, (to be published).
[16] K. Starosta, in *Nuclei at the Limits*, edited by T. L. Khoo and D. Seweryniak, AIP Conf. Proc. No. 764 (AIP, New York, 2005), p. 77.
[17] T. Koike *et al.*, Phys. Rev. Lett. **93**, 172502 (2004).
[18] I. Ragnarsson *et al.*, Hyperfine Interact. **43**, 425 (1988).
[19] K. Starosta *et al.*, Phys. Rev. C **65**, 044328 (2002).